

REPORT DOCUMENTATION PAGE			Form Approved OMB NO. 0704-0188	
Public Reporting burden for this collection of information is estimated to average 1 hour per response, including the time for reviewing instructions, searching existing data sources, gathering and maintaining the data needed, and completing and reviewing the collection of information. Send comment regarding this burden estimates or any other aspect of this collection of information, including suggestions for reducing this burden, to Washington Headquarters Services, Directorate for information Operations and Reports, 1215 Jefferson Davis Highway, Suite 1204, Arlington, VA 22202-4302, and to the Office of Management and Budget, Paperwork Reduction Project (0704-0188,) Washington, DC 20503.				
1. AGENCY USE ONLY (Leave Blank)		2. REPORT DATE 12 June 2005		3. REPORT TYPE AND DATES COVERED Final Report 01 Oct 02 - 30 Sep 04
4. TITLE AND SUBTITLE Collaborative Analysis of CASES-99 Lidar Data			5. FUNDING NUMBERS Agreement Number: DAAD19-02-1-0417	
6. AUTHOR(S) William Eichinger				
7. PERFORMING ORGANIZATION NAME(S) AND ADDRESS(ES) University of Iowa 300 Riverside Drive, Iowa City, IA 52242			8. PERFORMING ORGANIZATION REPORT NUMBER	
9. SPONSORING / MONITORING AGENCY NAME(S) AND ADDRESS(ES) U. S. Army Research Office P.O. Box 12211 Research Triangle Park, NC 27709-2211			10. SPONSORING / MONITORING AGENCY REPORT NUMBER 42980.1-EV	
11. SUPPLEMENTARY NOTES The views, opinions and/or findings contained in this report are those of the author(s) and should not be construed as an official Department of the Army position, policy or decision, unless so designated by other documentation.				
12 a. DISTRIBUTION / AVAILABILITY STATEMENT Approved for public release; distribution unlimited.			12 b. DISTRIBUTION CODE	
13. ABSTRACT (Maximum 200 words) This study deals with the analysis of CASES99 data. Specifically, with elastic and water vapor lidar data and supporting micrometeorological data from sonic anemometers, hygrometers, and long and short wave, upwelling and downwelling radiation fluxes. The analysis has two major parts. The first is the development of algorithms to obtain meteorologically useful information from the lidar data. This part of the study has been reasonably successful, and will generate a number of publications outlining the methods and analysis. This part also includes the discovery of a new type of inversion method that is quite successful. The second is the search for a theory to explain how gravity waves interact with the surface and result in vertical transport. This part of the study has resulted in a number of interesting observations, but has not resulted yet in a theory that will explain, mathematically, the processes that lead from one phenomenon to the resulting observations of vertical transport.				
14. SUBJECT TERMS Lidar, gravity wave, inversion, stable boundary layer			15. NUMBER OF PAGES	
			16. PRICE CODE	
17. SECURITY CLASSIFICATION OR REPORT UNCLASSIFIED	18. SECURITY CLASSIFICATION ON THIS PAGE UNCLASSIFIED	19. SECURITY CLASSIFICATION OF ABSTRACT UNCLASSIFIED	20. LIMITATION OF ABSTRACT UL	

NSN 7540-01-280-5500

Standard Form 298 (Rev.2-89)
Prescribed by ANSI Std. Z39-18
298-102

Enclosure 1

Collaborative Analysis of CASES-99 Lidar Data

Principal Investigator
William Eichinger
University of Iowa

Statement of the problem

The present state of knowledge about the formation of stable boundary layers and the transport of materials within it is incomplete and our ability to accurately model such conditions is poor. Yet these conditions are very important for a wide variety of reasons ranging from pollution control (most exceedances are associated with stable conditions) to chemical/biological defense. The problem is difficult at least in part because the atmosphere becomes horizontally stratified, requiring detailed measurements high up into the atmosphere where measurements of any kind are difficult. CASES-99 was a one month field program during which a wide variety of sensors were deployed to measure various atmospheric parameters during stable conditions. Data from three lidar systems (a miniature elastic scanning lidar, water Raman lidar and a vertical profiling lidar) and a conventional meteorological array were taken by the investigator as part of the CASES-99 experiment..

This project involved collaboration with other groups to analyze the data taken by the investigator and others in order to address the physics of stable boundary layers. The goal is to increase our understanding of how events occur in stable conditions and with this, increase our capability to model such conditions. The data taken by the lidars is especially important to the analysis in that these instruments enable us to make connections between events that occur higher up in the atmosphere and those that occur close to the surface that are responsible for vertical transport.

Summary of the Results

Efforts on this project have been primarily centered on two major areas. The first is the development of novel data analysis methods in order to extract more information from the lidar remotely sensed data. The second is an attempt to understand the evening of 13-14 October, 1999 during the CASES experiment. This was an evening of nearly continuous gravity waves. This evening offers two possibilities. The first is the understanding of how gravity waves work. Between the various instruments at CASES, an extraordinarily complete data set exists with which existing models of gravity

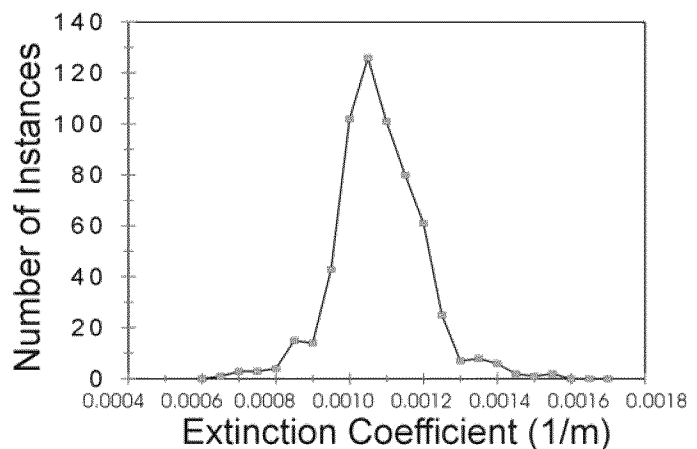


Figure 1. A plot of the probability distribution of attenuation coefficients for a single line of sight of the lidar during a rainstorm. A rainstorm is used as the example because the rain has a much greater reflectivity than the ambient air. Note the near Gaussian nature of the distribution.

waves can be tested. A comparison of the generated data with current theory was covered fairly completely by the paper by Fritts et al. (2003).

Data Analysis Methods

The efforts to extract meteorologically useful data from lidar measurements have produced a number of results. Estimates of the vertical velocity of the gravity waves was made by measuring the fluctuations in the height of the boundary layer. To do this, the height of the boundary layer had to be found in each of the separate lidar signals, each one second apart. This required the use of a consistent, yet robust algorithm. A search of the literature on the subject revealed a large number of algorithms, none of which were entirely satisfactory, were suitable for automated processing, or which would work in all cases. The results of the comparison of the various methods and the issues associated with the interpretation of the data will be submitted as a paper entitled, "Determination of the Height of the Boundary Layer by Lidar: A Review". An efficient and robust method was developed that is based upon a skimming technique used to find the boundaries of objects in photographs. This method will be the subject of a research note to be submitted. In working on the extraction of the wavelength and direction of the gravity waves from the scanning lidar data, a new type of inversion routine is being developed. Because the differences in the aerosol concentrations were extremely slight during CASES, removing noise and enhancement of the differences is important for a scanning lidar in which fewer laser pulses are averaged (so the signal to noise is less than for a staring lidar system). Conventional methods for inverting lidar data, such as the Klett method (Klett, 1981, 1985), require assumptions to be made for each line of sight. Because of this, inverted scanning lidar data is seldom shown because the results along each line of sight are inconsistent with the inverted data along adjacent lines of sight. Because the differences are so clear, inverted data has no credibility and is impossible to process

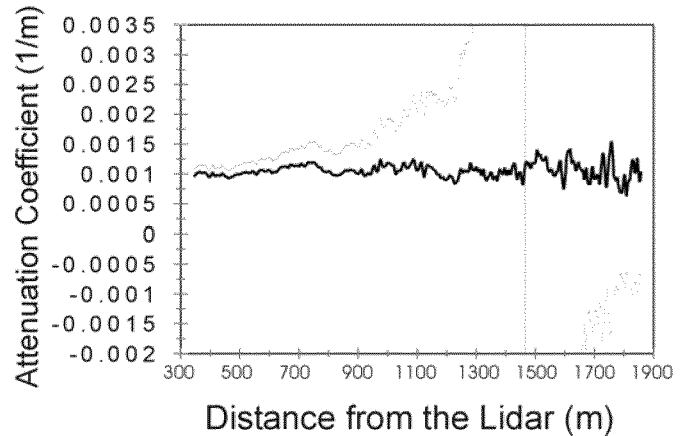


Figure 2. The attenuation coefficients obtained by inverting the lidar signal shown in figure 3 (the center line). Also shown are the attenuation coefficients obtained from inversions that assumed boundary condition values 5% larger and 5% smaller than the actual value. Note the sensitivity of the solution to the assumed boundary condition.

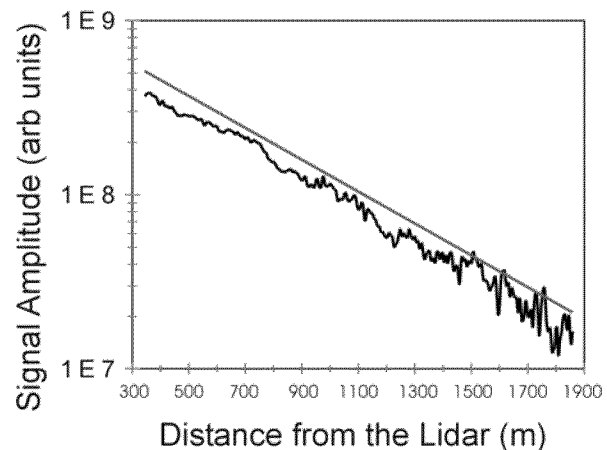


Figure 3. A semilog plot of the lidar signal used in the inversion analysis of figures 1 and 2. The straight line represents the slope of the average of the inverted attenuation coefficients. The degree of similarity between the two curves is an indicator of the effectiveness of the inversion.

further to obtain other parameters.

Examination of the data from CASES led to a method of inverting the data which attempts to minimize the variance of the inverted data. This is equivalent to assuming that the aerosol concentrations in a volume of space are normally distributed. While this has never been shown for aerosols, this property is known to be true for nearly all atmospheric measurements (temperature, water vapor concentration, wind speed, etc). The results of a successful inversion shown in figure 1 show a near-Gaussian distribution for the attenuation coefficients. The method was tested on synthetic lidar data and worked well for single component atmospheres, atmospheres in which there is only a single aerosol concentration distribution present (essentially the distribution of the background air, or in the case of figure 1, when some component of the air dominates the attenuation and backscattering). An example of a two component atmosphere would be one in which there was a plume from some source that was emitting nearby. The distribution of attenuation coefficients from the plume would also be normally distributed, but with a different mean value and width than that of the ambient air. It turns out that any number of distributions can be handled by the method, but each must be dealt with individually.

Classical lidar inversions (especially the forward solution) are notoriously sensitive to errors in the assumed boundary condition. The quality of the solution obtained by this method is shown in figure 2 which shows the inversion by this method (the center line) and the solutions from initial conditions that are just five percent higher and lower than the initial condition calculated by this method. Both of the perturbed solutions diverge significantly from the average value, differing by factors of three to five after only 1000 meters. The average value of the calculated attenuation coefficients is compared to the measured lidar signal in figure 3. The slope of lidar data plotted on a semilog plot can be used to estimate the average attenuation coefficient over a relatively long path. The similarity of the slope of the two curves is also an indicator of the reliability of the inversion method.

The difficulty with the method is that each distribution must be identified from the data, the physical locations of each distribution must be identified and then coefficients must be calculated for each line of sight for each distribution. Because of the number of lines of sight and the sheer amount of data in a single vertical (RHI) scan, the development of efficient algorithms is difficult. Work now centers on extending the method from a single line of sight to multiple lines of sight. We are also attempting to determine the theoretical reasons why the method works as well as it does. Although we anticipate publication of the method at a somewhat later date, work has begun on a draft of a paper on the basic method entitled, "A Constrained Lidar Inversion Routine". Because of the complexity associated with multidimensional scanning, the paper is not likely to be submitted until later this summer.

A summary of the data extracted and the methods used to extract it from lidar measured variables will be written as a journal article entitled, "Lidar Techniques for the Measurement of Gravity Wave Parameters in the Nocturnal Boundary Layer" to be submitted for publication.

Deposition of Energy from Gravity Waves

The second topic is the effect that gravity waves have on vertical transport. It was discovered during CASES that there is a relationship between vertical transport near the surface and the amplitude of the gravity waves (figure 4). One of the results of CASES has been demonstrations that events higher up in the atmosphere propagate down to the surface and affect vertical transport. As can be seen in figure 4, the maximum latent energy flux is a function of the amplitude of the gravity wave (as measured by the deflection of the top of the boundary layer) that is currently passing by. Alternately, the vertical

velocity of the wave could be used as a measure. While it makes sense that there is more energy in a large amplitude wave, gravity wave theory suggests that ducted waves should pass by without loss of energy from the wave (the amplitude of the wave and the vertical velocity at the surface should be zero). This theory however assumes a flat surface. Real surfaces have obstructions, trees, small hills and so on. These obstructions could be treated as perturbations of

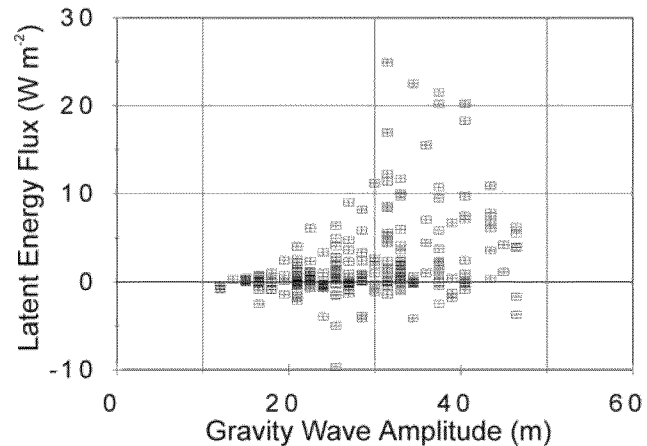


Figure 4. A plot showing the “instantaneous” vertical transport of water vapor to the gravity wave amplitude at the time.

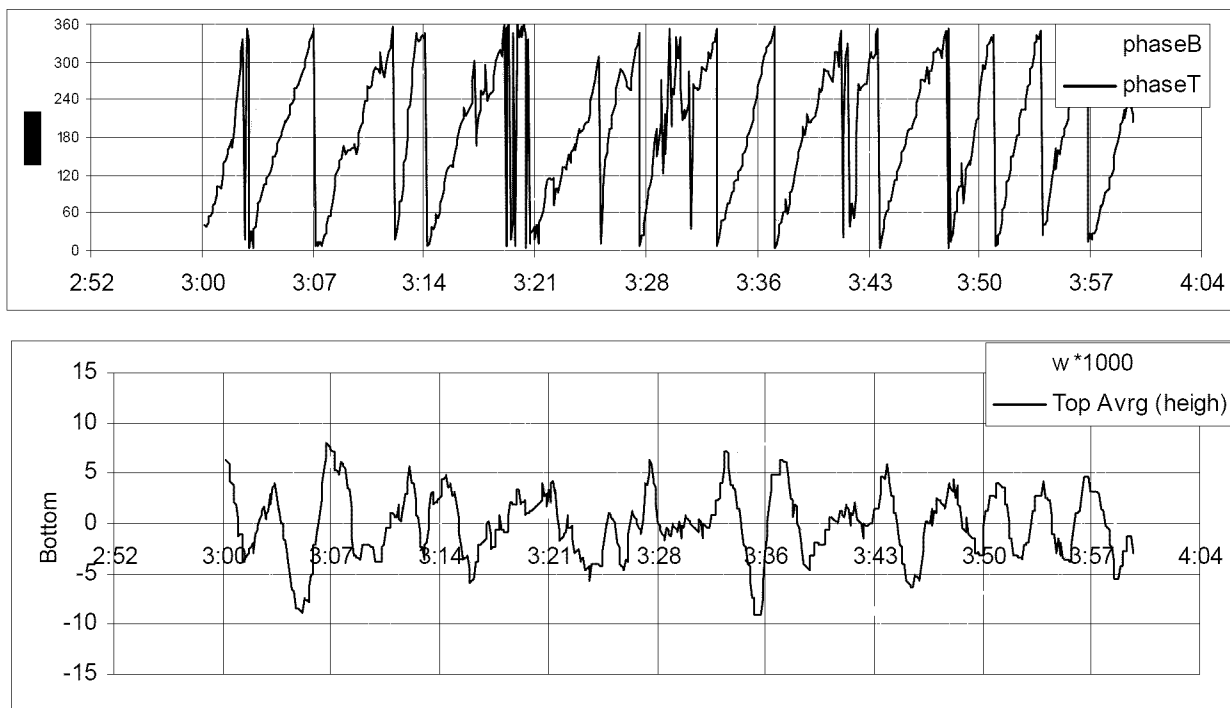


Figure 5. A plot of the phase relationships between the motion of the top of the boundary layer and the vertical velocity at an altitude of 2.3 m above the ground.

the basic wave. The interaction of the perturbed waves with the original wave and the mean flow should lead to increased turbulent kinetic energy and vertical transport.

We turned to electromagnetic theories for ducted waves for an explanation. Theories for the transport of microwave energy in waveguides is highly developed and is quite

similar to gravity wave theory (the biggest difference being that for gravity waves, the properties of the medium change with altitude). There is also a well-developed perturbation theory for these waves.

However, we have never been able to go from calculating the characteristics of the perturbed wave to the change in turbulent kinetic energy that would be caused by the perturbation. In atmospheric turbulence, the interaction of structures of different sizes (or in Fourier terms, wavenumbers) produces new structures that are the sum and difference of the original structures, and leads to a breakdown in wavenumbers that is the dissipation of kinetic energy. At present, we believe that the equations will have to be rewritten in Fourier space and solved in that form in order to achieve the desired information.

Sparked by an interest in chaos theory, we investigated the relationships between the wave amplitude at the top of the residual layer (as shown by the changes in the height of the residual layer), shown in blue and the vertical wind speed 2.3 meters above the surface shown in green on figure 5. There have been a number of recent papers on the effect of

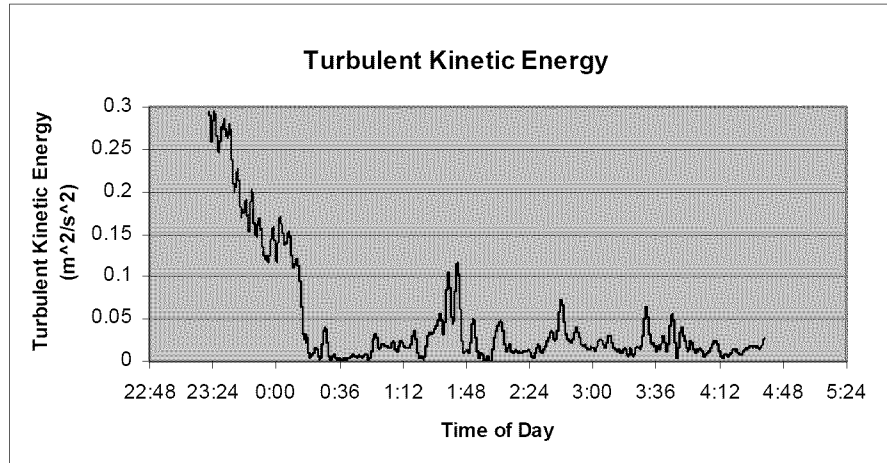


Figure 6. A plot of the turbulent kinetic energy as a function of the time of the evening. The data is for the evening of the 13/14 October, 1999 during the CASES99 experiment. The data is from the UI sonic anemometer array.

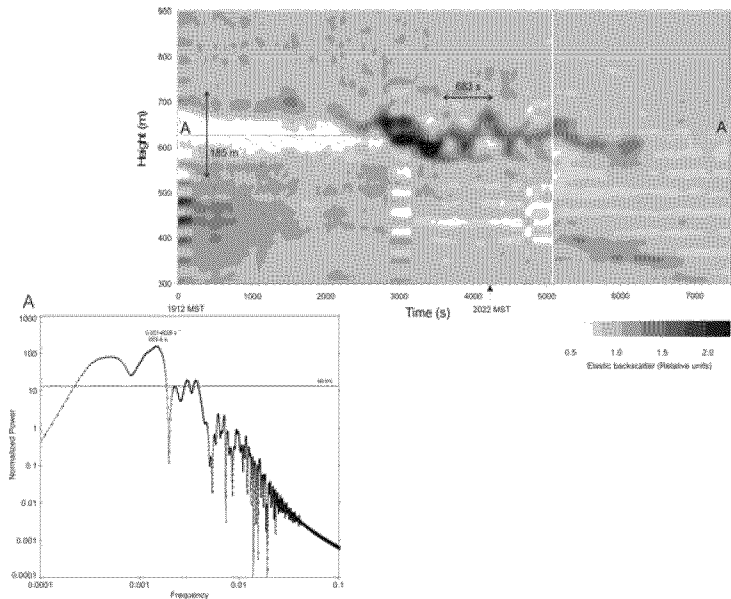


Figure 7. Vertical staring elastic lidar time-height scan for IOP-4 acquired at 2012 MST showing a potential wave structure between 600 m and 700 m. The wave length of the disturbance is approximately 683 s long, as defined by power spectrum analysis from data along transect A-A, and the depth of the disturbance is approximately 185 m. Inset A shows the power spectrum for data acquired along transect A, and a -5/3 slope line (dot) is shown for reference.

phase synchronization of weakly coupled self-sustained chaotic oscillators (for example, Rosenblum et al., 1996). These papers use an analytical signal approach based on the Hilbert transform and Poincaré maps. For coupled attractors, the phase relationships are maintained, while the amplitude of the states may vary chaotically and may seem uncorrelated to the eye. For much of the night of 13-14 October during CASES, the two waves are in phase. Occasionally they become out of phase with each other. Figure 5 is an example of a time when they are often out of phase with each other. For example, at 3:04 and 3:45, the two waves are out of phase.

Referring to figure 6, one can see that these times correspond to times with higher levels of turbulent kinetic energy (figure 6) (and thus increased vertical transport). Associated with times when the waves are out of phase are an increased period for the fluctuations in the vertical wind speed (the period is longer during these times). What causes this is unknown.

As in many cases with chaos theories, the analysis is descriptive and not predictive. Thus it is not likely that this line of attack will lead to a predictive analysis that will allow a mathematical description of how the breaking of a gravity wave leads to vertical transport. However, this kind of chaos theory predicts that when the phases are synchronized, it is the result of a state with a “macroscopic mean field”. In other words, the gravity wave remains intact when the phase of the waves at the top and bottom of the boundary layer remain synchronized.

Collaborating with investigators in Los Alamos, Univ. Of Georgia, and Oak Ridge, a study was done using VTMX data as well as CASES to look at transport in the lower part of the boundary layer. Using lidar data collected in the stable boundary layer, a representation of the processes responsible for the transport and exchange of water between the surface and the atmosphere can be obtained both spatially and temporally. The analysis that was accomplished suggested that the initial instability that generated the lidar observed structures originates above the SBL, from the presence of a local instability, which then produces the necessary set of conditions required to support various standing pressure or density waves such as K-H waves. These waves propagate to the surface, provided certain stability conditions are present within the atmosphere such as a waveguide. Small pressure perturbations can induce turbulence at the

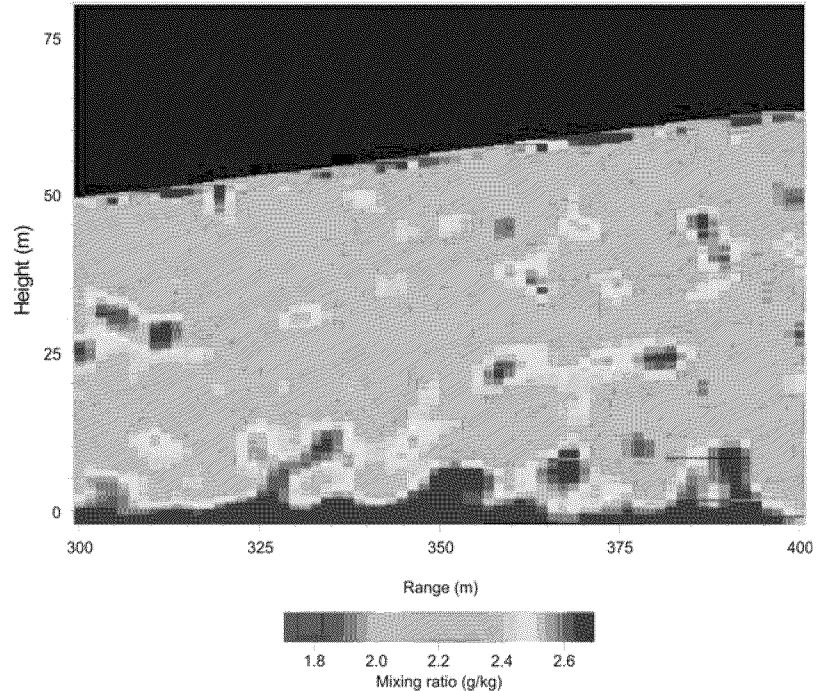


Figure 8. Range-height water-vapor scan from IOP-4, 2027 MST showing coherent structures and possibly a roll vortices, red is high water vapor and blue is low. The roll structure is between 20 and 25 m high.

surface.

The evidence for this mechanism in this study comes from both the lidar and point-sensor data including the elastic backscatter image (Fig. 7), the Raman lidar image (Fig. 8), and the vertical wind speed time-series, and the vertical wind speed power spectrum (Fig. 9). The elastic backscatter data shows a wave between 600 and 700 m, with a period of approximately 683 s as estimated by peak power spectrum analysis. Further, the growth and decay of a coherent structure occurs over a 10 scan period, equivalent to 540 s. The sonic anemometer w time series spanning 1200 s sampled at 10 Hz shows that there was a substantial decrease in w between 20:31 and 20:32 MST and another large negative fluctuation at 20:43 MST, approximately 696 s after the first episode. Further, the time series also shows at least two potential “ramp” structures of approximately 3.5 to 4 min long. Ramps are indicative of the passing of coherent structures, such as eddies and plumes, and have been observed in both the unstable and stable boundary layers. In addition, an FFT derived power spectrum of the w time series shows a peak frequency of $0.00186665 \text{ s}^{-1}$ or a period of 535 s. Independent estimates of the ITS from observations of the dissipation rate provided by a nearby scintillometer were also approximately 11 min to 12 min in duration, supporting the contention that a periodic process was occurring. The coincidence of the elevated wave structure period of approximately 11 min. and similar periods for the surface observed fluctuations in the w time series and dissipation rate, along with the birth and decay of the intermittent structures, strongly suggests that the intermittency at the surface of the stable boundary layer can be coupled to wave processes aloft.

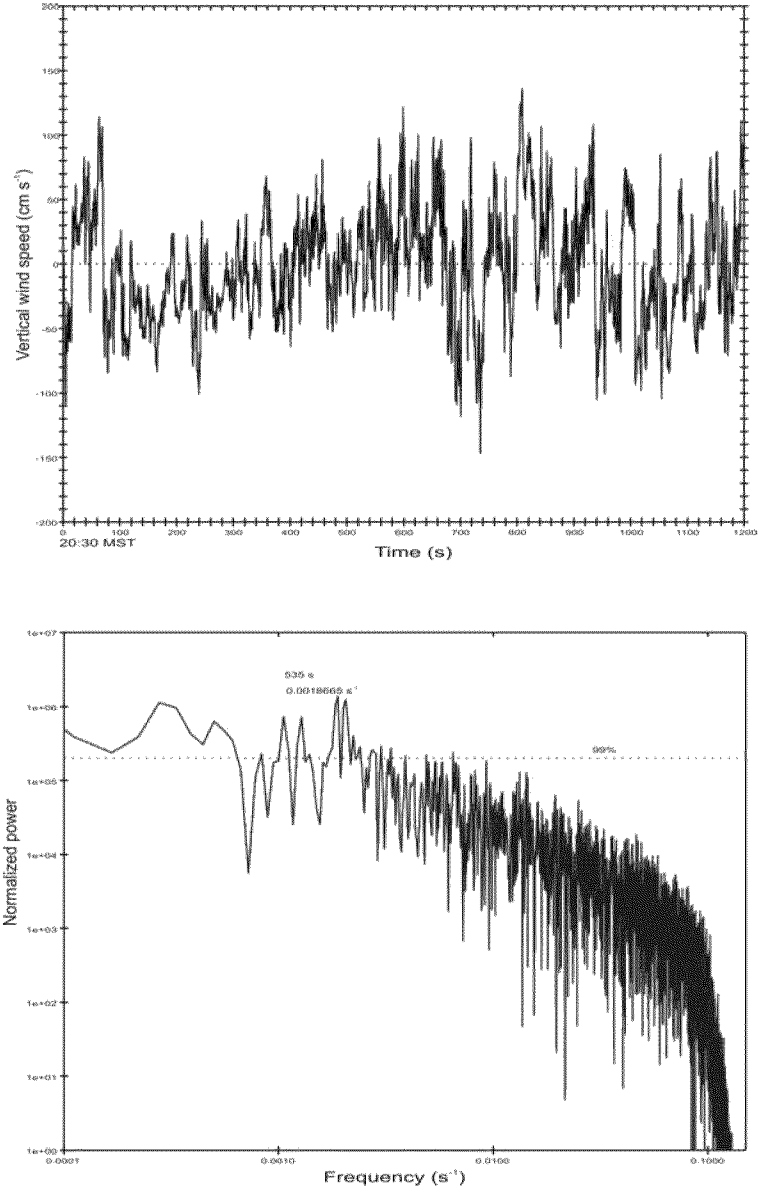


Figure 9. Vertical wind speed (w) time series acquired from a 3-axis sonic anemometer sampled at 10 Hz and smoothed with a 40 point averaging window acquired at 2030 MST on October 8, 2000. The time between major deviations in the time series is shown to be on the order of 11.6 min., as well as at least two potential ramp structures of 3.67 min in duration. Lower panel shows the normalized power spectrum of the w time-series along with the peak frequency equivalent to 8.9 min. and the 99% confidence interval.

There are reasonable indications that the microscale structures observed at the surface are coupled to wave properties several hundred meters aloft. At the time of this writing, a quantitative mechanism to show the coupling is not available. Independent vertical wind and scintillometer measurements acquired in the vicinity of the lidar showed distinct fluctuations associated in time with the onset of wave structures at 600 m above ground level. These fluctuations are roughly coincident in time with the microscale turbulence observed by the lidar, and are suspected of being the initiator of the local instability.

The results of this collaborative analysis was submitted to *Agricultural and Forest Meteorology* as a paper entitled, "Mass Exchange in the Stable Boundary Layer by Coherent Structures".

Listing of Publications Supported Under This Grant.

(a) Papers published in peer-reviewed journals

David C. Fritts, Carmen Nappo, Dennis M. Riggan, Ben B. Balsley, William E. Eichinger, and Rob K. Newsom, 2004, "Analysis of Ducted Motions in the Stable Nocturnal Boundary Layer During CASES-99", *Journal of the Atmospheric Sciences*, 60, 2450-2472.

(b) Manuscripts submitted, but not published

Cooper, D.I., M.Y. Leclerc, J. Archuleta, R. Coulter, W.E Eichinger, C.Y.J. Kao and C.J. Nappo 2005, Mass Exchange in the Stable Boundary Layer by Coherent Structures, *Agricultural and Forest Meteorology* 13X (2005) .

Eichinger, W., H. Holder, D. Cooper, J. Nichols, and E. Carlson, "Lidar Techniques for the Measurement of Gravity Wave Parameters in the Nocturnal Boundary Layer", for submission to *Journal of Atmospheric and Oceanic Technology*.

Eichinger, W., D. Cooper, and J. Nichols, "A Technique to Determine the Height of the Boundary Layer from Lidar Data", for submission as a research note to *Journal of Atmospheric and Oceanic Technology*.

Eichinger, W., D. Cooper, J. Nichols, and E. Carlson, "Determination of the Height of the Boundary Layer by Lidar: A Review", for submission to *Journal of Atmospheric and Oceanic Technology*.

Eichinger, W., and H. Holder, "A Constrained Lidar Inversion Routine", submitted to *Applied Optics*.

(c) Technical reports submitted to ARO

None

Scientific Personnel Earning Advanced Degrees While Employed on the Project

Renee Van't Land - Masters degree

Jennifer Nichols - Masters degree

Report of Inventions

No inventions from this project

Bibliography

David C. Fritts, Carmen Nappo, Dennis M. Riggin, Ben B. Balsley, William E. Eichinger, and Rob K. Newsom, 2004, "Analysis of Ducted Motions in the Stable Nocturnal Boundary Layer During CASES-99", *Journal of the Atmospheric Sciences*, 60, 2450-2472.

Klett, J. D. (1981), "Stable Analytical Inversion Solution for Processing Lidar Returns," Appl. Opt., **20**, 211-220.

Klett, J. D. (1985), "Lidar Inversion with Variable Backscatter/extinction Ratios," Appl. Opt. **24**, 1638-1643.

Measures, R. M. (1984), Laser Remote Sensing, John Wiley & Sons, Inc., New York, 510.

Michael G. Rosenblum, M.G., A.S. Pikovsky, and J. Kurths, 1996, "Phase Synchronization of Chaotic Oscillators", *Physical Review Letters*, **11**, 1804-1807.